Engineering & Performance of DuoTurbo: Microturbine with Counter-Rotating Runners

D. Biner[1], V. Hasmatuchi[1], D. Violante[1], S. Richard[1], S. Chevailler[1], L. Andolfatto[2] F. Avellan[2], C. Münch[1]

[1]University of Applied Sciences and Arts, Western Switzerland, Route du Rawyl 47, Sion, Switzerland.

[2]EPFL Laboratory for Hydraulic Machines, Avenue de Cour 33 bis, 1007 Lausanne, Switzerland

Email : daniel.biner@hevs.ch

Abstract. Considering the nuclear phase-out strategy of several European countries and the future tendency to promote renewable energies, the exploitation of small hydropower sites (<10 MW) becomes increasingly important. In this framework DuoTurbo Turbine, a new DuoTurbo-microturbine prototype for drinking water networks has been jointly developed by the HES-SO Valais//Wallis, the EPFL-Laboratory for Hydraulic Machines and industrial partners. The modular in-line "plug & play" technology requires low investment, reaching economic feasibility with an available power between 5 kW and 25 kW. One stage of the microturbine consists of two axial counter-rotating runners that form a compact independent unit. Each runner of the turbine holds its own rim generator, the DuoTurbo-configuration involving that each hydraulic runner is integral with each electrical rotor. The possibility of stacking several stages in series enables covering quite a wide range of hydraulic power and, thus, recovering a maximum of energy dissipated in release valves of water supply systems. The present work introduces the global concept of the implemented prototype of the DuoTurbo-microturbine, to target a maximal injected power of 5 kW for a discharge of 9 l/s and a head of 24.5 m per stage. The main features of the hydraulic, the mechanical, the electrical and the electronic design are presented. The hydraulic performance is, then, assessed using CFD simulations for the expected operating range. Finally, the performance measurements of the single-stage prototype installed in the hydraulic test rig of the HES-SO Valais//Wallis are presented.

1 Introduction

In Switzerland about 5.7 % of the electricity production is provided by small scale hydropower plants that refer to facilities with a gross capacity below 10 MW. Indeed, there are more than 1'300 small scale hydropower plants installed providing an annual electricity production of 3'400 GWh. A maximum estimated annual small hydro potential of 1'600 GWh is still unexploited [1]. In particular, hydropower of drinkable water makes a noticeable proportion of this untamed energy potential. Drinking water turbines offer many advantages in ecological and economical terms by benefiting from existing water supply networks and sales of eco-electricity. Especially in the alpine regions of Switzerland where about 42 % of the drinkable water comes from spring tapping, drinking water turbines are commonly installed. For drinking water installations with a head and a discharge lower

than 50 m and 10 l/s respectively, using conventional technologies is not economically viable. In this context, DuoTurbo, - a new microturbine for drinking water networks has been jointly developed by the HES-SO Valais//Wallis, the EPFL-Laboratory for Hydraulic Machines and industrial partners. Thanks to the compact design of this new hydro turbine, the costs of this system installed "in-line" are therefore minimal. Due to the adapted runner engineering and the multistage concept, a maximum of hydraulic energy dissipated in release valves can be recovered for quite a wide power range. One stage of the DuoTurbo-microturbine consists of two counter rotating runners and provides a nominal electrical output power of 6.7 kW for the actual prototype. No guide vanes are needed due to the two serial runners, whereby the rotational velocity of each runner is the degree of freedom to control the operating condition. Figure 1 shows a typical layout of a drinking water system supplied by spring tapping with an integrated microturbine. Two security elements protect the drinking water installations from overpressure and the microturbine from overload. The presented paper introduces the global concept of the implemented DuoTurbo-microturbine prototype, designed in view of the future test site in Savièse, VS Switzerland. First, the hydraulic, mechanical, electrical and electronical concepts are introduced. Then, the CFD simulations carried out to assess the hydraulic design performance are presented. The last part deals with the experimental investigations to measure the whole system efficiency.

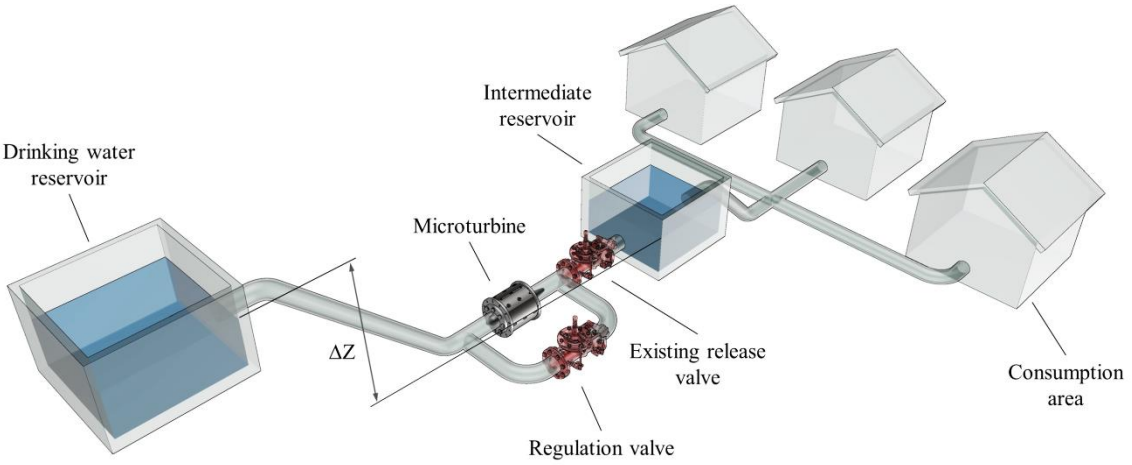

Figure 1. Layout of a drinking water system with integrated microturbine

2 General Concept

2.1 Hydraulic concept

The microturbine is a multistage axial reaction turbine with two serial counter-rotating runners per stage. The hydraulic design is based on the characteristics of the envisaged drinking-water facility and refers exclusively to the runner geometry. The drinking-water system of Savièse, VS Switzerland, where tests will be carried out in the future, is used as case study. This site experiences large variation of both head and discharge [2]. For the design of the runners, two operating conditions are selected: the nominal point and the maximum power, see Table 1. Considering the available hydraulic energy of the site, the maximal mechanical energy transferred by each runner can be determined. Assuming that the flow passing through the micro-turbine remains on a constant radius cylindrical surface, the Euler turbine equation applied to a given streamline yields the relation between the hydraulic specific energy transferred to the runners and the balance of angular momentum which depends on the flow direction and velocity. Assuming a purely axial flow at the inlet and as requested a purely axial flow at the outlet of the machine, the Euler turbine equation can be applied to determine the relative flow angles, see Figure 2. The profile shape is obtained by an indirect profiling method, defining a camber-line and

thickness distribution [3]. The camber line shape is thereby mainly determined by the relative flow angles. The minimal axial blade length is a parameter imposed by the mechanical requirements, in order to enable the mounting with the generator rim. The number of blades is chosen to prevent pressure field oscillations at the runner interface as well as to obtain a favourable blade density. The blade density is the ratio between the chord length and the blade pitch [4]. Choosing a blade density of 1.25 - 1.5 best results were obtained using this design approach. Adjustments of the geometry parameters have been made based on CFD simulations. The implementation of an optimisation algorithm is still in progress with the objective of maximizing the annual energy production considering the site characteristics and in particular the occurrence of the discharge.

Hydraulic parameters			
	Q_{nom}	**Q_{max}**	
Discharge	0.009	0.014	[m^3/s]
Specific hydraulic energy	240	~ 600	[J/kg]
Rotational speed 1st runner	-2'500	-3'500	[1/min]
Rotational speed 2nd runner	2'500	3'500	[1/min]
Hydraulic power	2'157	~ 8'385	[W]
Geometric parameters			
Shroud diameter	0.1		[m]
Hub diameter	0.08		[m]
Axial blade length	0.03		[m]
Number of blades 1st runner	3		[-]
Number of blades 2nd runner	5		[-]

Table 1. Main design parameters of the DuoTurbo-microturbine

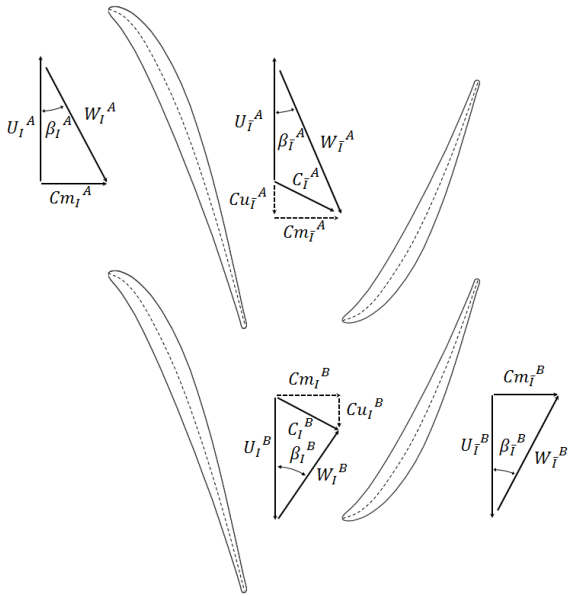

Figure 2. The hydraulic modelling is based on velocity triangles and camber-line with thickness. Indexes: $\square_{\bar{I}}$ low pressure reference section, $\square_I$ high pressure reference section, $\square^A$ first runner, $\square^B$ second runner

2.2 Mechanical concept

The development of a DuoTurbo-microturbine in this scale is an unknown area in many respects which is the key challenge of the project. Apart from the functionality, lifetime and efficiency, the production and maintenance costs must be minimized in view of an industrial fabrication, see also [5]. The implemented prototype serves as the basis for the following development steps. The mechanical conception of the DuoTurbo-microturbine is subject to the following technical requirements i.e. the compactness, the rotating parts concentricity, the bearing lifetime, tightness, materials compatibility, the minimization of volumetric losses. An overview of the mechanical components of the prototype is presented in Figure 3. The unit of the turbine runner and the rotor of the rim generator is the main feature of the DuoTurbo architecture. The rotating parts are thereby in contact with the passing fluid. In the generator's "*air gap"* a polymer tube is placed that separates the fluid region from the electrical parts. Each stator consists of two separable sheet metal bundles which enclose the polymer tube and guarantee the mechanical resistance against the pipeline pressure. Labyrinth seals minimize volumetric losses through the generator air gap. Ceramic ball bearings mounted on a central shaft take up the radial but mainly axial forces. A compact design with a total length of 526 mm per stage, including the diffusor and an outer diameter of 300 mm is realized at this stage.

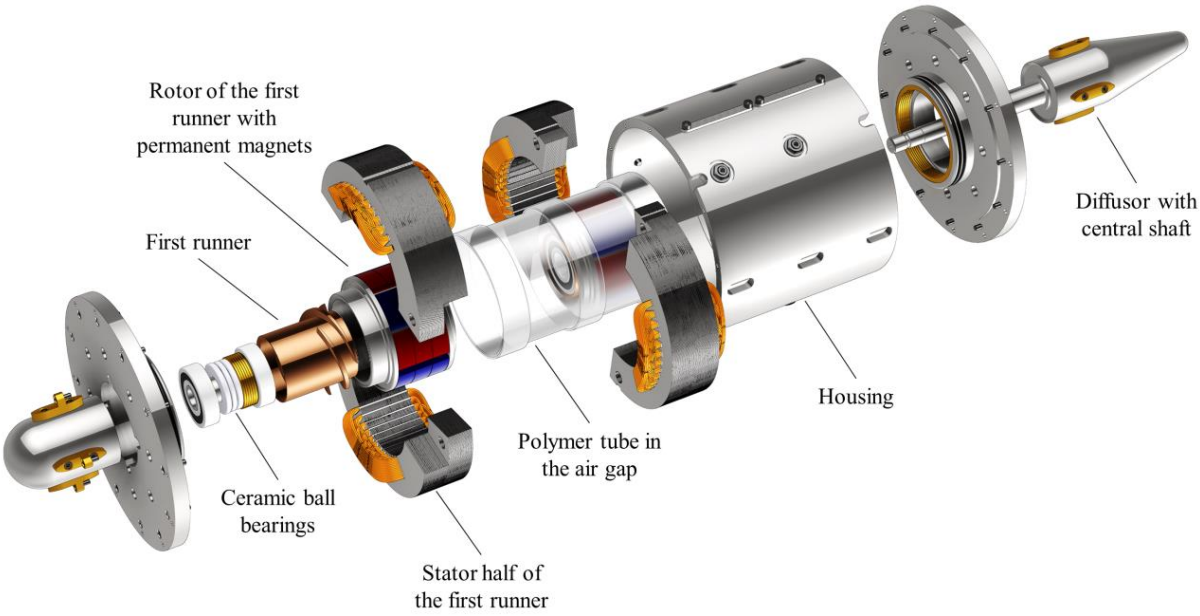

Figure 3. Mechanical concept of the DuoTurbo-microturbine prototype

2.3 Electrical concept

The DuoTurbo architecture has required the complete development of custom-made permanent magnet synchronous rim generators [6], as illustrated in Figure 4. The generator specifications underlie the requirements imposed by the hydraulic characteristics and dimensional restrictions, see Table 2. A principal design step is the determination of the generator topology that is defined by the number of poles, the number of slots, and the number q of slots per pole and per phase. FEM simulations using ANSYS Maxwell® [7] have been carried out to validate the performances during the design phase. Minimal torque ripple is obtained choosing $q = 2$, reaching an average dynamic torque of about 10.25 Nm at the nominal point. Neodymium magnets are used for the rotor made of eight poles. Since the runner distance is very small, the windings are distributed only over half the circumference (2×90°) of each stator, in order to minimize the distance between the generators and avoid a conflict between the generator end windings. For the nominal point a generator efficiency η_g of 92 % could be verified by experimental tests, reaching a nominal electrical power of 3.37 kW per generator. The global measured efficiency is shown in Figure 5.

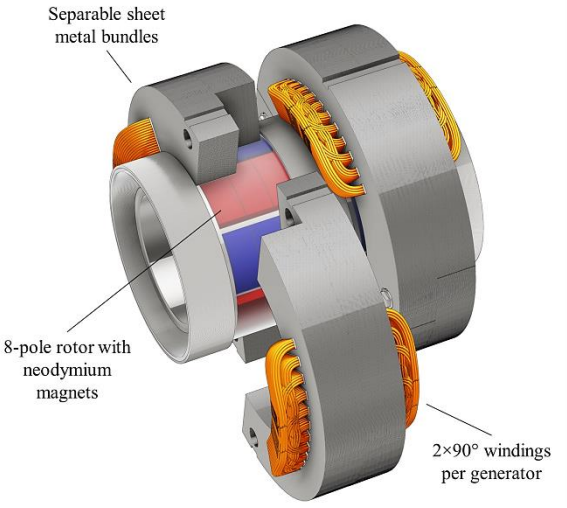

Figure 4. Geometry of the PM generator

Inner rotor diameter D_{ri}	100	[mm]
Outer rotor diameter D_{re}	126	[mm]
Mechanical air gap g	2.9	[mm]
Nominal rotational speed n	3'500	[1/min]
Nominal electromagnetic torque T_{em}	10	[Nm]
Line voltage U_l	400	[V]

Table 2. Technical specifications of the DuoTurbo-generators

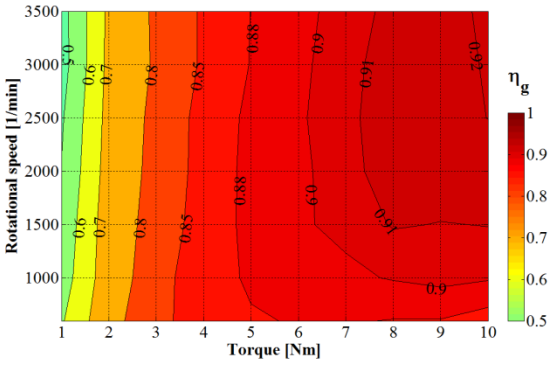

Figure 5. Measured generator efficiency

2.4 Power electronics

M700 Emerson converters have been used as a control system for variable speed of the two generators, as well as for the injection system to the electrical network of the laboratory. A converter on network side allows synchronization and injection to the power grid of the energy produced by the microturbine. Two converters on generator side control the variable speed of each turbine runner. The principal components of the power electronics are shown in Figure 6. The three Emerson modules are interconnected by a DC bus. This arrangement ensures operation in DRIVE mode and REGEN mode, into a four-quadrant converter that can control the two independent generators. The mechanical construction of the DuoTurbo-microturbine does not allow for mounting an encoder, consequently the variable speed control of the generators is made in sensorless mode.

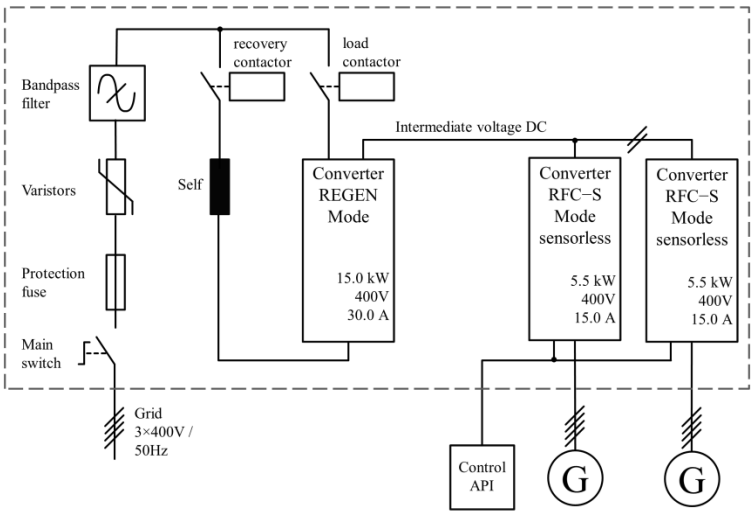

Figure 6. Electrical scheme of the power electronics

3 Performance of the DuoTurbo-microturbine

3.1 Numerical Simulation

3.1.1 Numerical Setup

The performance of the designed runners has been analysed over the whole operating range using 3D flow simulations of the reduced water passage of the DuoTurbo-microturbine. Only one stage has been considered at this state, see [8]. The steady state numerical simulations have been performed with the commercial software ANSYS CFX® 15.0 [9], based on the finite volume method. The SST turbulence model [10] was used and a convergence criterion RMS_{max} of 10^{-6} imposed. To limit the computational time the maximal number of iterations was set to 500 per operating point for tracing the global turbine

characteristic, whereby good convergence is obtained. A 2nd order spatial scheme with specified blend factor 1 was used. The software solves both the incompressible Unsteady Reynolds Averaged Navier-Stokes URANS equations in their conservative form and the mass conservation equation [11].

3.1.2 Spatial Discretization and Computational Domains

Reduced computational domains were used to minimize the computational time, since the evaluation of numerous operating points was targeted. The computational domain is shown in Figure 7, composed of four subdomains: the stator inlet domain, the inter-blade channels of the first and the second runner and the outlet domain. Structured meshes have been generated with the ANSYS ICEM CFD® commercial software. Information about the meshes is given in Table 3.

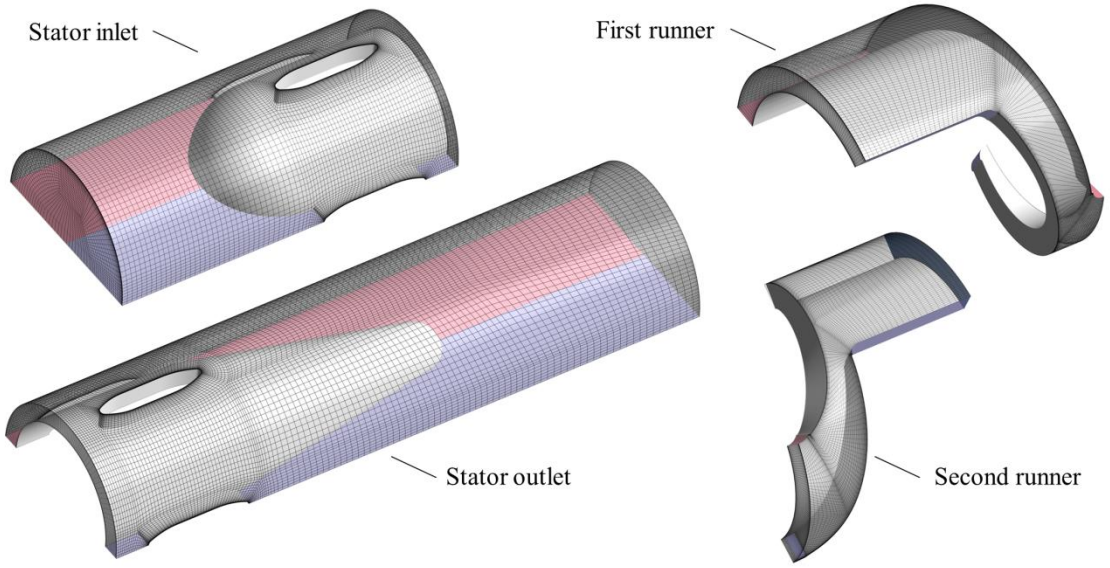

Figure 7. Computational domains and spatial discretisation

Domain	Mesh type	Nodes	Elements	Min. angle	y^+_{mean}	y^+_{max}
Stator inlet	Structured hexahedral	305’999	288’866	31.1°	10.78	28.06
Stator outlet		441’325	419’086	31.0°	11.01	45.65
First runner		310’794	292’545	38.4°	25.47	74.40
Second runner		268’906	252’813	28.9°	19.42	54.79
Total		1’327’024	1’253’310	-	-	-

Table 3. Mesh statistics (Values of the non-dimensional wall distance y^+ refer to the nominal point)

3.1.3 Boundary Conditions

Either the discharge or the relative pressure has been imposed at the inlet of the computational domain. At the outlet the gauge pressure has been set to zero. Due to the reduced domains, a rotational periodicity had to be defined at all periodic sections. A no-slip wall condition has been applied for all physical surfaces. The three domain interfaces are all of type frozen rotor. The boundaries are shown in Figure 8.

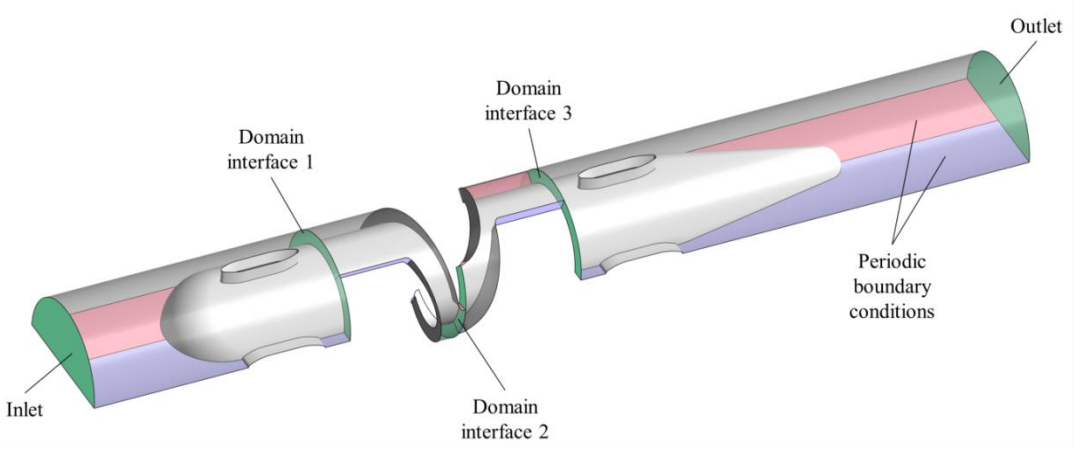

Figure 8. Boundaries and domain interfaces

3.1.4 Numerical Results

The results presented in Table 4 refer to the two main operating points as specified in part 2.1. The specific energy at the design point is closely matching the target value of 240 J/kg. For the second operating point the hydraulic energy transferred is higher than expected. A well balanced partition of the specific energy is obtained for both points. The total specific energy and consequently the hydraulic power are based on the complete machine, referring to the inlet and outlet of the simulated domain. The mechanical power and consequently the energetic efficiency takes into account the mechanical work produced by the runner blades. Very low recirculation and a nearly axial downstream flow are obtained as set out in the velocity streamline plot of Figure 9. The indicated normalized relative velocity W^* is the quotient of the relative velocity W and the meridional velocity Cm_{pipe} at the upstream water pipeline section.

Discharge	**1st runner specific energy**	**2nd runner specific energy**	**Total specific energy**	**Hydraulic power**	**Simulated mechanical power**	**Energetic efficiency**
Q	E_A	E_B	E_{tot}	P_h	P_m	η_e
[$m^3 \cdot s^{-1}$]	[$J \cdot kg^{-1}$]	[$J \cdot kg^{-1}$]	[$J \cdot kg^{-1}$]	[W]	[W]	[-]
0.009	130	116	250	2’240	2’007	0.90
0.014	316	335	661	9’222	8’113	0.88

Table 4. CFD simulation results for the main operating points.

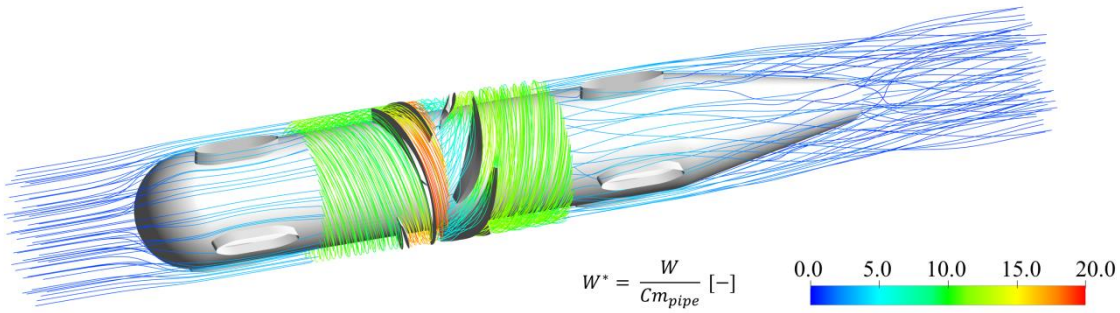

Figure 9. Instantaneous relative velocity streamlines at the design point

4 Experimental validation

4.1 Hydraulic Test Rig

At the University of Applied Sciences HES-SO Valais/Wallis, a hydraulic test rig has been installed to perform tests of small scale turbines, pumps and other hydraulic components [12]. The test rig is built on two floors and supplied with fresh water from a main reservoir. Three recirculating multistage centrifugal pumps with variable speed are connected in parallel to supply the water circuit with hydraulic power. A maximal discharge of 100 m^3/h and a maximal pressure of 160 mWC can be delivered. A pressurized reservoir allows simulating different implantation levels of the model that serves for cavitation investigations. An automatic regulation system controls the operation of the test rig through a customized LabView® interface. The rotational speed of the pumps, the head on the testing model and the discharge can therefore be regulated. A wireless architecture has been implemented for the data communication. The actual prototype of the DuoTurbo-microturbine has been installed and tested on the test rig, as shown in Figure 10.

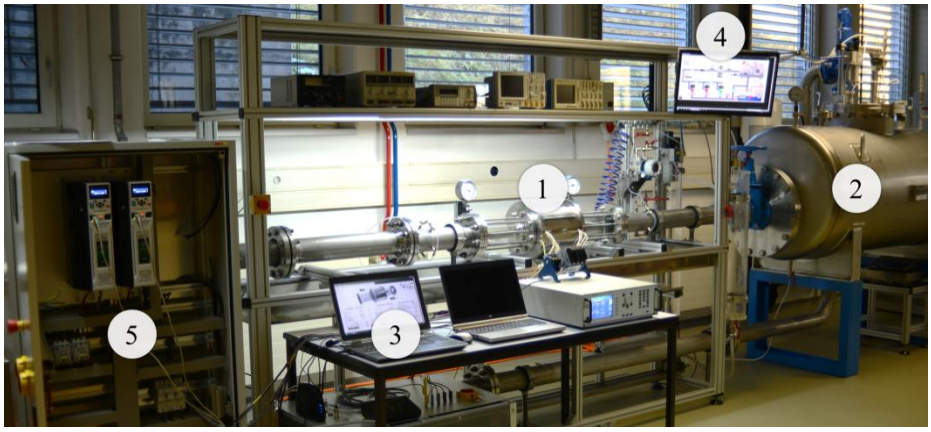

Figure 10. Hydraulic test rig of the HES-SO Valais//Wallis with the installed DuoTurbo-microturbine prototype. 1) DuoTurbo-microturbine prototype 2) Downstream pressurized reservoir 3) Control interface of the microturbine 4) Control interface of the test rig 5) Generators driving and regenerating power electronics

4.2 Testing Method

The experimental measurements have been performed at constant testing head, while the rotational speed of the runners along with the speed ratio α (1) were varied. Setting the desired head, the system automatically adjusts the pumps rotational speed in order to reach and stabilize the target value. The head is measured on the basis of the static pressure at the inlet and outlet of the microturbine. Since only the effective torque transmitted by the electrical generator rotor can be captured, only the total resulting mechanical power P_{m_tot} can be measured (2). The measured efficiency η_{h-m} is therefore composed of the mechanical efficiency η_m and the hydraulic efficiency η_h. Further, the hydraulic efficiency is composed of the energetic efficiency η_e, the volumetric efficiency η_q referring to the leakage through the labyrinth seals and the disc friction efficiency η_{rm} referring to viscous friction of the rotating parts (3). Since a detailed analyses and modelling of the different losses has not been realized at this point, the validation of the numerical results in terms of efficiency is not possible.

$$\alpha = \frac{n_A}{n_B} = \frac{\omega_A}{\omega_B} \quad (1) \qquad \eta_{h-m} = \eta_h \cdot \eta_m = \frac{P_{m\_tot}}{P_h} \quad (2) \qquad \eta_h = \eta_e \cdot \eta_q \cdot \eta_{rm} \quad (3)$$

n_A: First runner rotational frequency, n_B: Second runner rotational frequency

4.3 Experimental results

In order to obtain the final global efficiency characteristic of the turbine, several sets of measurements have been first performed at constant testing head, varying the rotational speed of each runner from 0 to 3500 1/min. The normalized total mechanical power $P_m{}^*$ at a constant head of 4 bar is represented as a function of the runners rotational speeds in Figure 11, the final H-Q-η_h* (4) hill chart being provided in Figure 12.

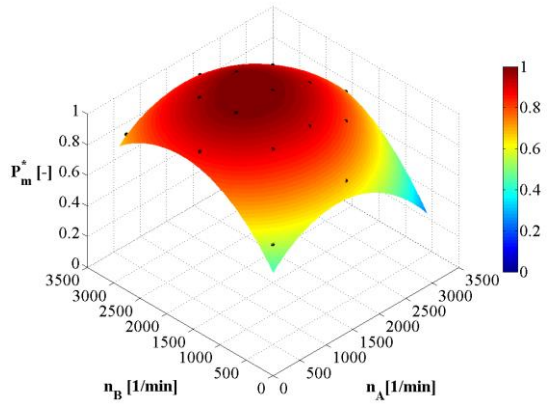

Figure 11. Hill chart of the measured n_A-n_B-P_m* characteristics for a head H of 4 bar

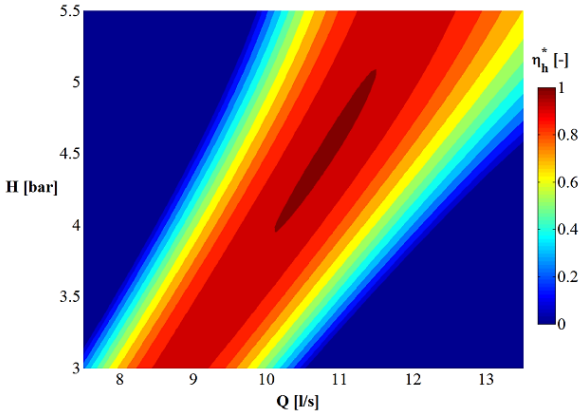

Figure 12. Hill chart of the measured H-Q-η_h* characteristics

$$\eta_h{}^* = \frac{\eta_{h-m}}{max(\eta_{h-m})} \quad (4) \qquad P_m{}^* = \frac{P_{m\_tot}}{max(P_{m\_tot})} \quad (5)$$

4.4 Comparison of numerical and experimental results

The following results refer to CFD simulations and measurements performed at a constant speed ratio of 1. The energy coefficient ψ depending on the discharge coefficient φ obtained by numerical simulation and by experimental measurements are compared in Figure 13. Indeed, these coefficients can be compared since they do not depend on the mechanical power. The fact that there is no significant difference between the numerical and experimental results allows anticipating that the volumetric losses in the generators rotor-stator gap are minimal.

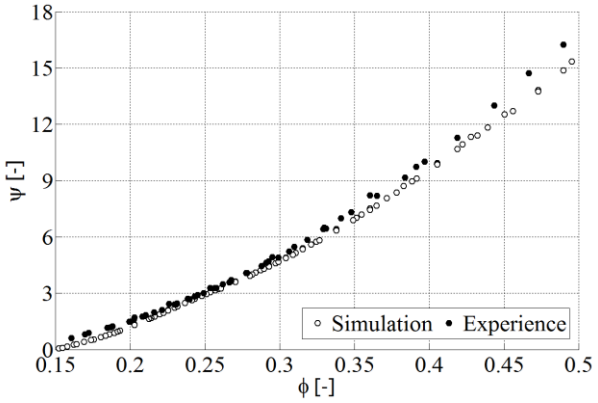

Figure 13. φ - ψ characteristics of numerical and experimental results

5 Conclusion

In the context of small hydropower exploitation of drinking water supply networks, a prototype of a new DuoTurbo-microturbine has been successfully developed. The compact multistage concept enables an "in-line" installation for low investment costs and thus profitable exploitation of hydraulic power between 5 kW and 25 kW. A specific development for the hydraulic, mechanical, electrical and electronic concepts has been carried out. In particular, custom made permanent magnet synchronous generators with high efficiency have been developed. Due to the variable discharge of drinking water systems, two main operating points were specified in view of the future prototype test site. Steady state numerical flow simulations confirm the targeted hydraulic properties and an efficient blade design. Experimental investigations have been carried out on the hydraulic test rig of the HES-SO Valais//Wallis and confirmed the functionality of the developed system. The φ - ψ characteristic found by numerical simulations was also confirmed by the experimental tests. A detailed analyses and modelling of the different losses are ongoing to complete the design assessment.

Acknowledgements

The research leading to the results published in this paper is part of the KTI DuoTurbo project number 17197.1 PFEN IW, supported by the Swiss Commission for Technology and Innovation. This project is performed in the framework of SCCER Supply of Electricity. The authors would like to thank to the industrial partners Telsa SA, Valelectric Farner SA and Jacquier-Luisier SA for their collaboration.

References

[1] "Bundesamt für Energie BFE," 2012. [Online]. Available: http://www.bfe.admin.ch. [Accessed 12 02 2016].

[2] L. Andolfatto, E. Vagnoni, V. Hasmatuchi, C. Munch-Alligné and F. Avellan, "Simulation of energy recovery on water utility networks by a micro-turbine with counter-rotating runners," in *IAHR*, Grenoble, 2016.

[3] D. Biner, V. Hasmatuchi, F. Avellan and C. Münch-Alligné, "Design & Performance of a hydraulic micro-turbine with counter rotating runners," in *5th International Youth Conference on Energy*, Pisa, Italy, 2015.

[4] R. Rey and R. Noguera, "Profils, grilles d'aubes et machines axiales," Paris, 2008.

[5] L. Andolfatto, C. Euzenat, E. Vagnoni, C. Münch-Alligné and F. Avellan, "A mixed standard/custom design strategy to minimize cost and maximize efficiency for Picohydro power potential harvesting," in *5th International Youth Conference on Energy*, Pisa, Italy, 2015.

[6] D. Violante, L. Farner and S. Chevailler, "Design of a PM generator," HES-SO Valais//Wallis, Sion, 2015.

[7] ANSYS Maxwell, Version 15.0.0, ANSYS Maxwell User's Guide, ANSYS Inc, 2014.

[8] C. Münch-Alligné, S. Richard, B. Meier, V. Hasmatuchi and F. Avellan, ""Numerical simulations of a counter rotating micro turbine"," *Advances in Hydroinformatics, P.Gourbesville et al. (eds.), Springer Hydrogeology,* pp. 363-373, 2014.

[9] ANSYS CFX, release 15, ANSYS CFX User's Guide, ANSYS Inc, 2015.

[10] Menter, F.R., "Two-equation eddy viscosity turbulence models for engineerign application," in *AIAA Journal 32(8)*, vol. 32, 1994, pp. 1598-1605.

[11] Launder B.E., Spalding, D.B., "The numerical computation of turbulent flow," in *Computer Methods in Applied Mechanics and Engineering 3(2)*, 1974, pp. 269-289.

[12] V. Hasmatuchi, S. Gabathuler, F. Botero and C. Münch, "Design and control of a new hydraulic test rig for small hydro turbines," *Hydropower & Dams,* vol. 22, no. 4, pp. 54-60, 2015.